THE JOURNAL OF PHYSICAL CHEMISTRY B

Article

pubs.acs.org/JPCB

Can Surface Hopping sans Decoherence Recover Marcus Theory? Understanding the Role of Friction in a Surface Hopping View of Electron Transfer

Martin J. Falk, Brian R. Landry,* and Joseph E. Subotnik

Department of Chemistry, University of Pennsylvania, 231 South 34th Street, Philadelphia, Pennsylvania 19104, United States

ABSTRACT: We compare the dynamics of Fewest Switches Surface Hopping (FSSH) in different parameter regimes of the spin-boson model. We show that for exceptional regions of the spin-boson parameter space, FSSH dynamics are in fact time-reversible. In these rare instances, FSSH does recover the correct Marcus rate scaling (as a function of diabatic coupling) without the addition of decoherence. In regions where dynamics are irreversible, however, FSSH does not recover the correct Marcus rate scaling. Finally, by comparing the friction dependence of rates predicted by various decoherence schemes to an analytic result by Zusman, we provide yet more evidence that the method of introducing decoherence has a qualitative effect on the accuracy of results and this effect must be treated carefully.

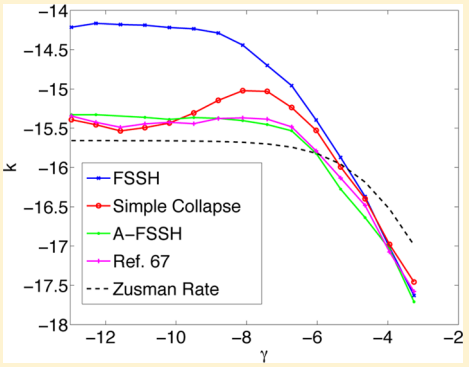

1. INTRODUCTION: THE FSSH ALGORITHM, FRICTION, AND THE DECOHERENCE CONUNDRUM

Classical approaches to molecular dynamics have been quite successful in simulating dauntingly complex interactions, particularly in the context of protein motion[1−3] and calculations of properties of liquids.[4−6] However, these methods confine themselves to the ground-state Born−Oppenheimer potential energy surface and are therefore unable to account for nonadiabatic effects. Given the importance of nonadiabatic transitions,[7,8] there has been and will continue to be an interest in producing algorithms that go beyond the Born−Oppenheimer approximation.[9−17] While numerical integration of Schrodinger's equation is possible in principle, it is rarely feasible for systems with more than a handful of degrees of freedom. Thus, a wide variety of attempts have been made to bridge the gap between classical approaches and fully quantum solutions. Among methods which focus on accounting for nonadiabatic electronic transitions, Tully's Fewest-Switches Surface Hopping (FSSH)[18] algorithm has emerged as a popular platform in recent years.[19−22] However, FSSH does not necessarily reproduce certain qualitative predictions made by chemical theory,[23−28] and many of the major divergences of FSSH from theory can be attributed to the decoherence problem.[29−39] Specifically, FSSH fails to account fully for the loss of coherence among electronic degrees of freedom. In general, decoherence is a phenomenon that arises when a quantum subsystem is coupled to a larger environment. In the context of FSSH, features of decoherence appear when particles move through multiple regions of derivative coupling, or the same region multiple times.[28]

One specific consubstantiation of this decoherence occurs when considering the Marcus theory result for the spin-boson model.[40] Marcus theory predicts that, in the limit of small diabatic coupling (V), the rate of transfer from one well to the other should be proportional to the square of the diabatic coupling. However, our group recently showed that FSSH does not recover this result; for a finite-temperature, spin-boson model, quadratic scaling is recovered only when decoherence is incorporated into FSSH.[41] That being said, Sibert et al. have recently provided evidence suggesting that FSSH can sometimes recover the correct V^2 scaling of the zero temperature transition rate.[22]

Thus, it appears as if the incorporation of decoherence is crucial in certain regimes of the spin-boson model, but not in others. In this paper, we seek to understand how and why this is the case. What relevant characteristics distinguish these two regimes, and how should we modify FSSH to account for this? As this paper will show, the distinguishing factor that causes the incorrect scaling of rate with respect to V is the time-reversibility of the dynamics. Furthermore, the specific way in which we attempt to correct for the effects of decoherence also has implications for the accuracy of our predictions.

We outline our paper as follows: First, we discuss the theory behind our implementation of FSSH and our model system, and describe the specific procedures used to measure transition rates and electronic behavior. Second, we present our data, and observe trends between the time-reversibility of the evolution of the system under FSSH, our methods of incorporating decoherence, and the accuracy of the results as compared to Marcus theory. Finally, we clarify the implications of our

Special Issue: James L. Skinner Festschrift

Received: January 31, 2014
Revised: April 7, 2014

   dx.doi.org/10.1021/jp5011346 | J. Phys. Chem. B XXXX, XXX, XXX−XXX

observations for the data from Sibert et al. and suggest conditions for when and how decoherence must be accounted for in surface hopping style algorithms.

2. METHODS

2.1. Spin-Boson Model and FSSH Notation. Our model system for studying FSSH is the spin-boson model, which has frequently been used as a simplified representation of electron transfer.[11,42,43] It has been studied recently with FSSH,[19,41,44] and previously with other surface hopping algorithms.[45,46] In a diabatic basis, the spin-boson model describes two parabolic energy wells together with a diabatic coupling V. This system is then modeled as being in contact with a bath of harmonic oscillators at a well-characterized temperature T. More precisely, we have the following Hamiltonian:

$$\mathcal{H} = \begin{pmatrix} \frac{1}{2}m\omega^2 x^2 + Mx & V \\ V & \frac{1}{2}m\omega^2 x^2 - Mx - \epsilon_0 \end{pmatrix} \tag{1}$$

where V is the diabatic coupling between the two states ("left" $|\Xi_l\rangle$ and "right" $|\Xi_r\rangle$), m is the mass of the nuclear coordinate, ω is the natural frequency of the system, ϵ_0 is the driving force, and M is related to the reorganization energy via $M = ((1/2)\ E_r m\omega^2)^{1/2}$. In the context of electron transfer, one of the diabatic energy wells is representative of an electron donor, and the other an electron acceptor. As written, eq 1 involves only one nuclear degree of freedom, x. In general, when desirable, we will incorporate a bath of nuclei through the addition of a fractional parameter γ. This corresponds formally to a quantum Brownian oscillator spectral density.[47,48]

Since we will run FSSH dynamics on adiabats, we diagonalize the Hamiltonian, obtaining the upper and lower adiabatic energy surfaces:

$$E_1(x) = \frac{1}{2}m\omega^2 x^2 - \frac{1}{2}\epsilon_0 - \sqrt{\left(\frac{1}{2}\epsilon_0 + Mx\right)^2 + V^2} \tag{2}$$

$$E_2(x) = \frac{1}{2}m\omega^2 x^2 - \frac{1}{2}\epsilon_0 + \sqrt{\left(\frac{1}{2}\epsilon_0 + Mx\right)^2 + V^2} \tag{3}$$

as well as the derivative coupling:

$$\mathrm{d}_{12}(x) = \frac{1}{2}\frac{MV}{\left(\frac{1}{2}\epsilon_0 + Mx\right)^2 + V^2} \tag{4}$$

We can also calculate the eigenvectors of our Hamiltonian, and from there write down the unitary change of basis matrix for transforming from the diabatic representation to the adiabatic representation. If we denote our upper and lower adiabatic states as $|\Phi_1\rangle$, $|\Phi_2\rangle$, then:

$$\begin{pmatrix} \mathcal{U}_{l1}(x) & \mathcal{U}_{r1}(x) \\ \mathcal{U}_{l2}(x) & \mathcal{U}_{r2}(x) \end{pmatrix} = \begin{pmatrix} \langle \Xi_l|\Phi_1\rangle & \langle \Xi_r|\Phi_1\rangle \\ \langle \Xi_l|\Phi_2\rangle & \langle \Xi_r|\Phi_2\rangle \end{pmatrix} \tag{5}$$

$$= \begin{pmatrix} \sqrt{\frac{1}{2} - \frac{1}{2}\frac{\frac{1}{2}\epsilon_0 + Mx}{\sqrt{(\frac{1}{2}\epsilon_0 + Mx)^2 + V^2}}} & -\sqrt{\frac{1}{2} + \frac{1}{2}\frac{\frac{1}{2}\epsilon_0 + Mx}{\sqrt{(\frac{1}{2}\epsilon_0 + Mx)^2 + V^2}}} \\ \sqrt{\frac{1}{2} + \frac{1}{2}\frac{\frac{1}{2}\epsilon_0 + Mx}{\sqrt{(\frac{1}{2}\epsilon_0 + Mx)^2 + V^2}}} & \sqrt{\frac{1}{2} - \frac{1}{2}\frac{\frac{1}{2}\epsilon_0 + Mx}{\sqrt{(\frac{1}{2}\epsilon_0 + Mx)^2 + V^2}}} \end{pmatrix} \tag{6}$$

Surface hopping trajectories are always propagated on adiabatic surfaces, with each trajectory carrying its own electronic wave function $(c_1,\ c_2)$ in an adiabatic basis. Recently,[49,50] our group has demonstrated that the correct means to evaluate diabatic populations via FSSH trajectories is to transform the FSSH fully nuclear-electronic density matrix into a diabatic basis—which requires information about the active surface for each trajectory as well as knowledge about each trajectory's electronic wave function. For the case of very small V, however, adiabatic and diabatic states are nearly identical, so that such a density-matrix procedure is unnecessary. In this case, instead, one can simply use the following rule:

- If a trajectory is moving on the i^{th} *adiabatic* surface, then the probability that the trajectory is moving on the a^{th} *diabatic* surface is $|\mathcal{U}_{ai}|^2$.

This interpretation will be used below and is valid when E_r is large and V is small; this interpretation corresponds to using the surface data only in the work of Shi et al.[48]

Finally, again in the limit of small V, for the purpose of analysis only, it will be helpful to convert the electronic wave function coefficients between adiabatic and diabatic bases. In this case, defining 1,2 as adiabatic indices and l,r as diabatic indices (for left and right wells), we can write

$$\begin{pmatrix} c_1 \\ c_2 \end{pmatrix} = \begin{pmatrix} \mathcal{U}_{l1} & \mathcal{U}_{r1} \\ \mathcal{U}_{l2} & \mathcal{U}_{r2} \end{pmatrix} \begin{pmatrix} c_l \\ c_r \end{pmatrix} \tag{7}$$

2.2. Choosing Parameters. By considering the average time it takes for a swarm of trajectories to transition from one diabatic well to the other, we can calculate a physically meaningful rate of decay. However, we first need to find allowable parameter regimes and physically sensible initial conditions for these trajectories.

As usual for all initial value representations, initial conditions for surface hopping calculations were chosen on the basis of a phase-space approximation of a nuclear wave function contained in the donor well. To determine this wave function, we took the Wigner transform of the ground state of a harmonic oscillator. We then considered each point in phase space as the initial condition of some classical trajectory, and from this association calculated a distribution of initial energies for our trajectories. However, instead of drawing the initial conditions of our trajectories from over the entirety of the distribution, we followed Sibert et al. and looked separately at how individual energies within this ground-state distribution behaved.[22] The values of initial energies E_i (relative to $-1/4E_r$, the minimum of the initial diabatic well) were chosen as the 40-quantiles of this distribution. These can be calculated as $E_i = -1/2\hbar\omega\ \ln(1 - (i/40))$ for $i = 0,...,39$. Having fixed E_i, we picked the initial positions and momenta from a microcanonical ensemble of energy E_i.

In order to study the effects of a stochastic force on the dynamics of FSSH, we also simulated interaction with a thermal bath at an effective temperature T_{eff}, following Tully and Beeman.[51,52] At every time step we added an additional term to the force on the trajectory in the form of $-\gamma p + \eta$, where γ is the Langevin friction term, and η is a random variable with a Gaussian distribution of mean $\mu = 0$ and standard deviation $\sigma = ((2\gamma m k T_{\text{eff}})/(\mathrm{d}t))^{1/2}$. Note that this T_{eff} does not correspond to an actual physical temperature, but rather was introduced in order to track the effect of stochasticity at various energies and to help us discern how particles with distinct energies (as drawn from the ground-state distribution) behaved. To be precise, if

dx.doi.org/10.1021/jp5011346 | J. Phys. Chem. B XXXX, XXX, XXX−XXX

we draw initial conditions from a microcanonical ensemble with an energy E_i, we chose our effective temperature T_{eff} such that the time-average energy will be equal to E_i.

The parameters ranges we used are listed in Table 1. When generating results to compare with Sibert et al., constants such as mass m, ω, and the reorganization energy E_r were chosen such that they would be as similar as possible to the quantities used in ref 22, used for modeling vibrations of the methyl dimer. Because we wanted to explore the Marcus regime, our choices for m, ω, and E_r then determined the appropriate ranges for the frictional Langevin coefficient γ: $(\omega(E_r kT_{\text{eff}})^{1/2}/V \gg \gamma \gg (V^2)/(E_r kT_{\text{eff}})^{1/2}$.[41]

Table 1. Parameter Ranges (in atomic units, $\hbar = 1$)

parameter	range
E_r	2.39×10^{-2}
E_i	$0-1.22 \times 10^{-3}$
kT_{eff}	9.5×10^{-4}
ϵ_0	2.2×10^{-2}
V	$2.5 \times 10^{-5}-1.00 \times 10^{-4}$
ω	6.64×10^{-4}
γ	$0.0-8.0 \times 10^{-4}$
m	2.92×10^{4}

Since increasing the driving force ϵ_0 increases the energy barrier to crossing from one diabatic state to another, and slows down calculations, ϵ_0 was chosen to be close to the barrierless regime. However, we were reluctant to be exactly in the barrierless regime, since we sought to avoid too many trajectories starting within the coupling region. Hence we chose $\epsilon_0 = 2.2 \times 10^{-2}$ to be close (but not too close) to the reorganization energy $E_r = 2.39 \times 10^{-2}$.

To identify the appropriate range for V, we note that, if we wish to use Marcus theory as a point of comparison, V must be small enough such that the Landau–Zener parameter $\alpha_{\text{LZ}} = (2\pi V^2)/(\hbar v|F_l - F_r|) \ll 1$. Here, v is the velocity with which a trajectory enters the crossing region, and F_r, F_l are the forces on the left and right diabatic surfaces, respectively, at the crossing point.[53] For the spin-boson model, if we are in a regime with a finite effective temperature, α_{LZ} can be estimated as $(2\pi V^2)/(\hbar\omega\ (2kT_{\text{eff}}E_r)^{1/2}$. In the $T_{\text{eff}} = 0$ case, trajectories all have a fixed energy E_i, in which case $\alpha_{\text{LZ}} = (2\pi V^2)/\hbar\omega\ (4(E_i - 1/4E_r)E_r + 2\epsilon_0 E_r - \epsilon_0^2)^{1/2}$.[54] Note that α_{LZ} will never be imaginary because we require that the trajectories have enough energy to pass the crossing point, so that $E_i > (\epsilon_0^2)/(4E_r) - 1/2\epsilon_0 + 1/4E_r$. Since the smallest E_i we chose was greater than 6.5×10^{-5} and the largest V was 0.0001, $\alpha_{\text{LZ}} \leq 0.06$, and we are firmly in the regime of Marcus theory.

2.3. Computation Details. To extract transition rates, we looked at the population of trajectories moving on the left diabatic surface as a function of time, and averaged over 10000 trajectories. Trajectories ran for a time of 2,000,000 atomic units with a time step of $dt = 0.25$ au. We then numerically fit this curve to an exponential decay, and from this process determined the decay constant. In order to prevent the system from periodically returning to its initial state in the zero friction limit, we halted trajectories that reached the minimum of the right well. Effectively, we are considering the lower adiabatic surface to be a dissociative surface, or equivalently, looking only at the rate of the first crossing from one diabatic well to the other. This choice is the precise situation that Sibert et al. simulate in their paper.[22]

To fit our population curves to an exponential decay, we used MATLAB to perform a least-squares regression on the logarithm of our data. However, difficulties arose when our population curves exhibited transient nonexponential behavior where the initial decay was relatively slow. This behavior disappeared by the time 20 percent of the trajectories had crossed from one diabatic surface to the other, and so in cases where this behavior arose, we simply ignored data from these earlier times. More oscillatory behavior occasionally lingered beyond this time period, but these oscillations did not interfere with extracting a rate of decay.

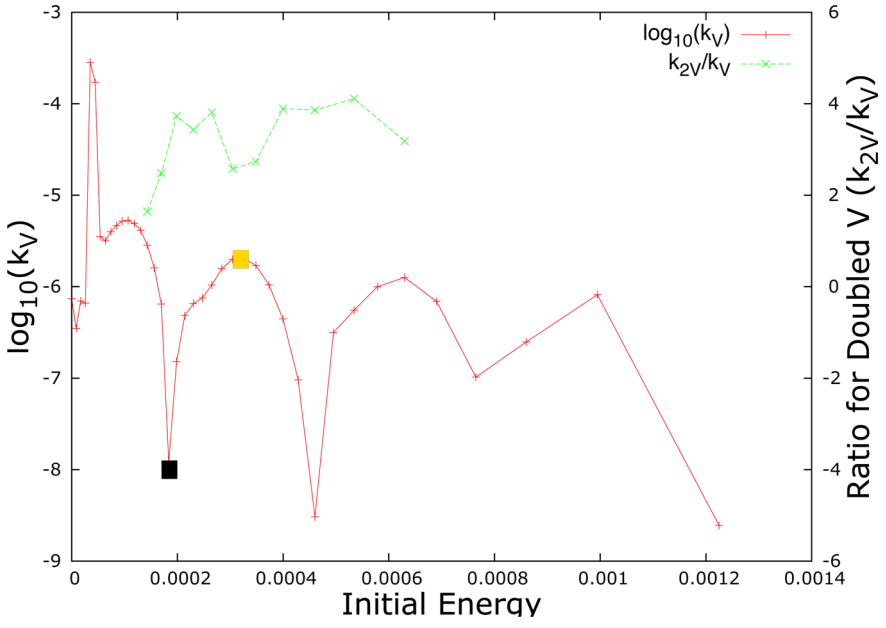

Figure 1. Red, left axis: zero friction transition rate (k_V) as a function of initial energy (relative to the minimum energy of the left diabatic well) at $V = 2.5 \times 10^{-5}$. Green, right axis: $(k_{2V})/(k_V)$, the relative transition rate obtained by doubling V, i.e. $V \rightarrow 2V$. For the meaning of yellow and black squares, see Figure 2

dx.doi.org/10.1021/jp5011346 | J. Phys. Chem. B XXXX, XXX, XXX–XXX

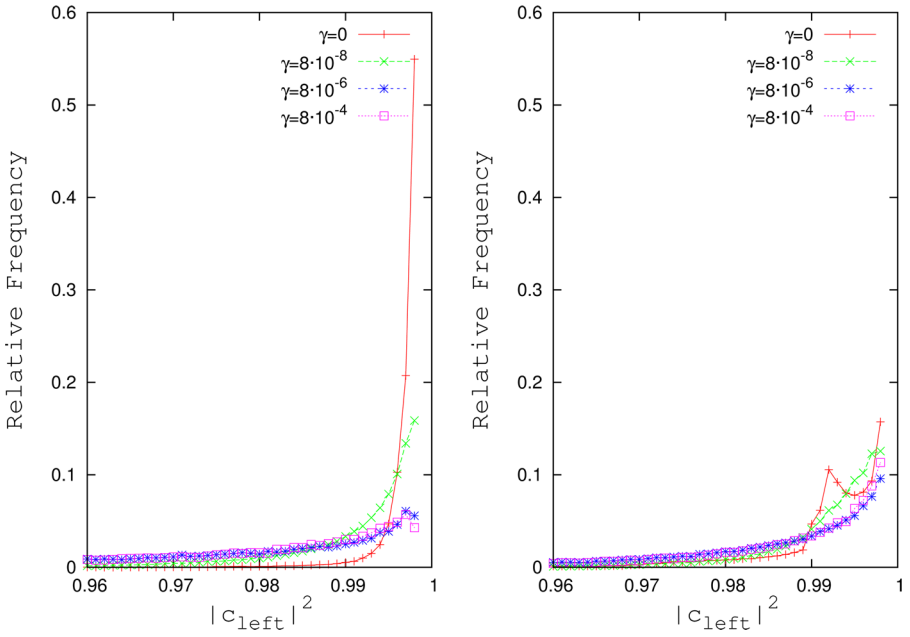

Figure 2. (Left) Frictional (γ) dependence of relative frequency of the magnitude sqaured of the wave function component $|c_l|^2$ corresponding to probabilities on the left diabat as measured at the minimum of the well. $E_i = 1.8 \times 10^{-4}$, near a local minimum on the plot of k_V as a function of E_i (see Figure 1, black square). (Right) Same plot as for the left, but now with energy $E_i = 3.5 \times 10^{-4}$, which corresponds to a local maximum on the plot of k_V as a function of E_i (see Figure 1, yellow square). $V = 2.5 \times 10^{-5}$.

To study the electronic dynamics of the system as predicted by FSSH, we recorded the electronic amplitudes for one diabatic surface each time a trajectory passed the minimum of the left well. More specifically, we calculated (c_l, c_r) as described in section 2.1. Then over the course of 2000 trajectories, with a time step of 0.25 au, we recorded $|c_l|^2$ every time a trajectory passed the minimum of the left well. At this point, measurements were plotted in a histogram with bin size of 0.001; bin sizes were chosen so that we had convergence in our distribution.

3. RESULTS

Our overarching goal in this paper was to determine the role friction plays in FSSH. We were motivated specifically by the Sibert study showing that the correct quadratic scaling of transition rate with respect to V in the spin-boson model had been recovered by FSSH in the zero friction limit.[22] However, this correct scaling had only been recovered for certain initial energies. Hence, we first searched for differences in the transition rate as a function of initial energy. The results of this procedure are plotted in Figure 1 in red.

The very fast rates observed at the very lowest energies ($E_i < 6.39 \times 10^{-5}$) are the result of frustrated hops; these trajectories have enough energy to escape the left well, but not enough to move to the upper surface in the absence of coupling to the environment. At larger energies, Figure 1 displays that, with zero friction, there are two distinct types of energies with respect to transition rate. At certain energies, the rate sharply decreases by about 2 orders of magnitude, while at most other energies the rate remains within the same order of magnitude.

To better understand the oscillations (in red) in Figure 1, we next considered the behavior of the electronic wave function in these two energy regimes. As described in section 2, we measured $|c_l|^2$, the magnitude squared of the component of the electronic wave function corresponding to the left diabatic well, each time a trajectory passed through the minimum of the left diabatic well. These measurements were subsequently plotted in histograms. As Figure 2 (Left) shows, at energies corresponding to a low transition rate, the distribution of measurements is sharply peaked. Furthermore, Figure 2 (Right) shows that for energies corresponding to a high transition rate, the distribution of wave function values is comparatively not as smooth and is much less peaked. Note that in both graphs, as friction increases, the distribution of values spreads out.

Figure 2 suggests that FSSH dynamics are time-reversible only with zero friction and only at certain initial energies. For these very particular circumstances, we would expect that the normalized distribution of $|c_l|^2$ as a trajectory crosses a fixed position to be a delta function. While Figure 2 (Left) is not exactly a delta function, its width in $|c_l|^2$ is nevertheless quite small in comparison to Figure 2 (Right). (The nonvanishing width of the distribution re-emphasizes the sensitivity of the dynamics with respect to the initial energy; if we differ slightly from a truly special energy, our dynamics will not be exactly periodic.) This suggests that the evolution of the total wave function is periodic (to within a certain tolerance) as it oscillates in the well. Hence dynamics going forward in time must be indistinguishable from dynamics propagating backward in time. In all other regions of our parameter space, there is a preferred direction for time. In regimes with random forces and friction, there is a clear culprit; the stochasticity and damping of the thermal and frictional forces result in a vanishingly small chance of the trajectories periodically returning to their initial conditions. In the zero-friction limit, FSSH-simulated dynamics also usually become time-irreversible because the periods for the real-space oscillations do not line up with the periods of the wave function oscillations. Hence, as time progresses, the small differences in the wave function value measured at the bottom of the diabatic well build up, and hence, the swarm of particles drifts further and further away from its initial configuration.

Finally, we may now compare the scaling of the rate with respect to V. From Marcus theory considerations, we should

dx.doi.org/10.1021/jp5011346 | J. Phys. Chem. B XXXX, XXX, XXX−XXX

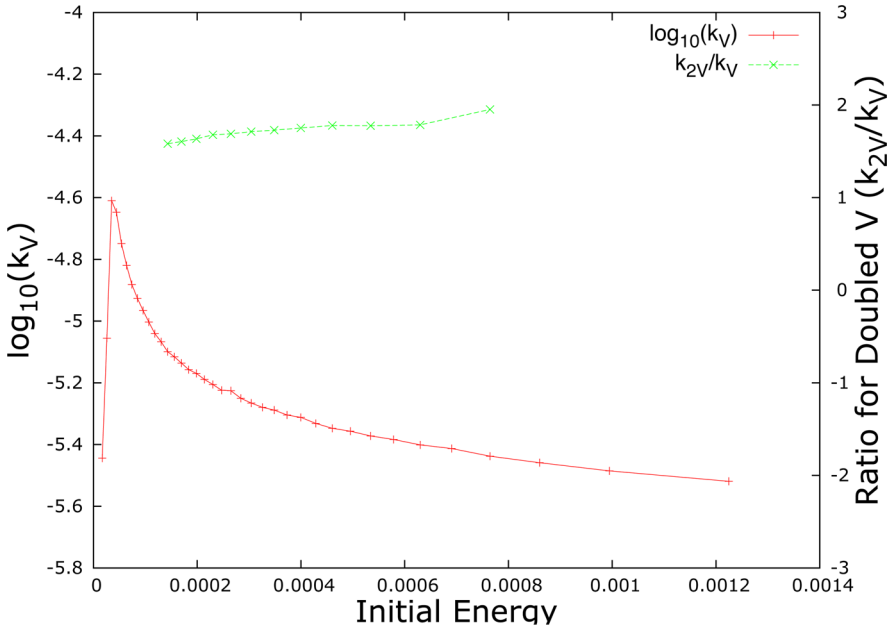

Figure 3. (Red, left axis) Finite friction ($\gamma = 8 \times 10^{-6}$) transition rate ($k_V$) as a function of initial energy (measured from the minimum of the left diabatic well) at $V = 2.5 \times 10^{-5}$. (Green, right axis) $(k_{2V})/(k_V)$, the relative transition rate obtained by doubling V, i.e. $V \rightarrow 2V$.

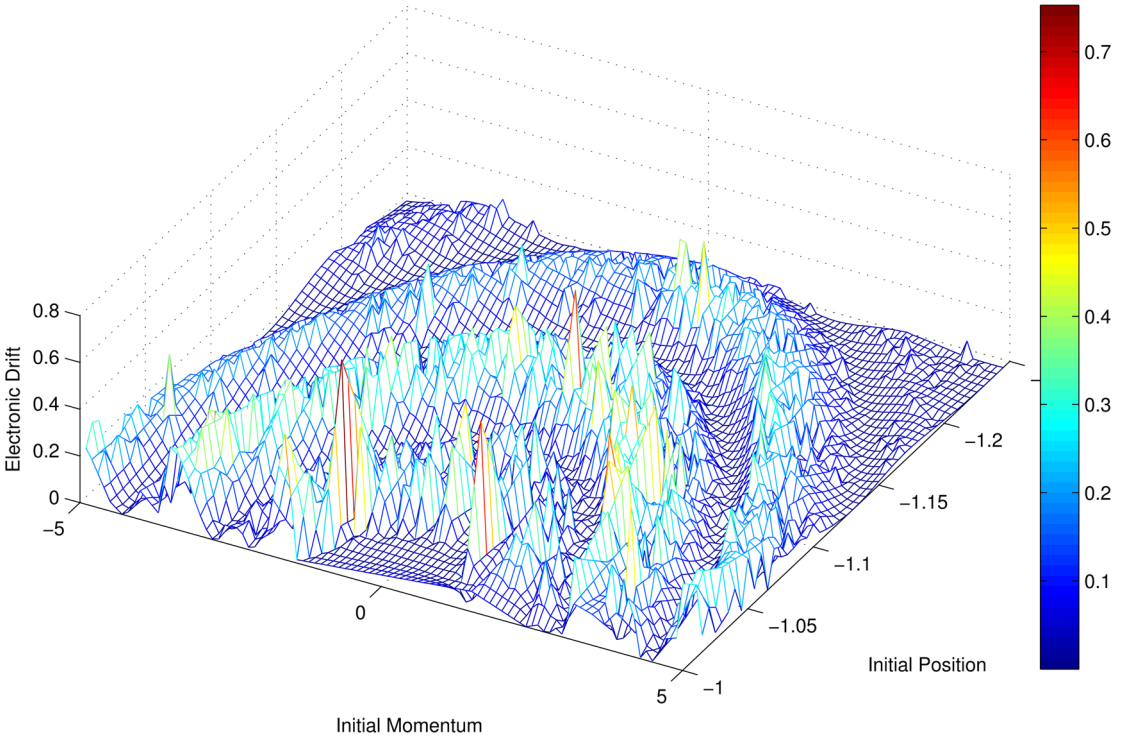

Figure 4. Drift in $|c_i|^2$ of a single trajectory after a time corresponding to five oscillations in a Morse potential well, plotted as a function of initial conditions. The diabatic coupling V is 1.0×10^{-4}.

expect that rates should scale as V^2. To determine a rough estimate of the scaling, we computed the rate at $V = 2.5 \times 10^{-4}$. Then, holding all other parameters constant, we doubled V. For the zero friction regime, results of this procedure are displayed in Figure 1 in green, superimposed on the plot of rate as a function of initial energy. Notice that $k_{2V}/k_V = 2$ near maxima of k_V, while $k_{2V}/k_V = 4$ near minima of k_V. Thus, our provisional conclusion is that, at energies for which the dynamics simulated by FSSH are time-reversible, the escape rate is proportional to V^2, while at energies where the dynamics are far from time-reversible, the escape rate is proportional to V.

For additional evidence of this claim, we also generated an analogue of Figure 1, but in a finite friction regime. We repeated the process that produced Figure 1, but instead of setting $\gamma = 0$, we let $\gamma = 8 \times 10^{-6}$. From Figure 2, we know that the dynamics are always time irreversible with $\gamma > 0$. The ratio k_{2V}/k_V is plotted in Figure 3. Of particular note for our purposes is the absence of resonant, oscillatory behavior in the

dx.doi.org/10.1021/jp5011346 | J. Phys. Chem. B XXXX, XXX, XXX−XXX

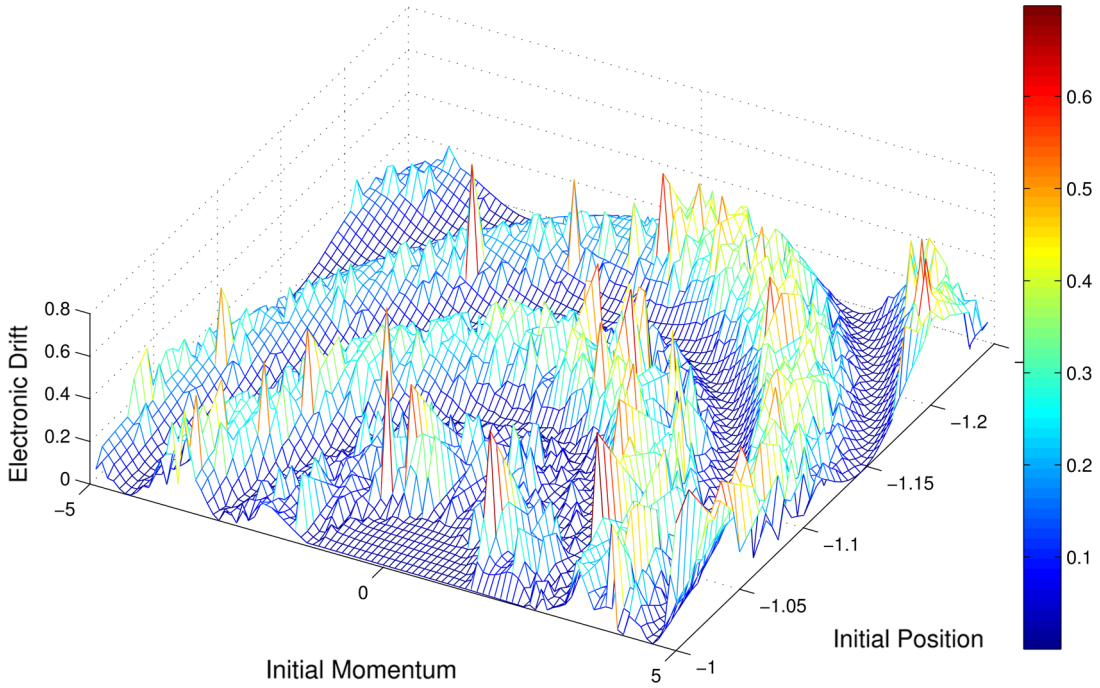

Figure 5. Drift in $|c_l|^2$ of a single trajectory after a time corresponding to five oscillations in a harmonic potential well, plotted as a function of initial conditions. The diabatic coupling V is 1.0×10^{-4}.

rates seen in Figure 1, and the failure of FSSH to recover V^2 scaling at all initial energies. Thus, we find again that only at those energies and frictional values ($\gamma = 0$) for which FSSH dynamics are time-reversible do we recover the correct result.

In the end, for chemists studying FSSH dynamics, Figures 1, 2, and 3 make intuitive sense. To correct FSSH to account for decoherence, most schemes collapse the electronic wave function with some algorithm-dependent rate. These collapsing events are essential to recovering V^2 scaling within the context of time-irreversible dynamics. However, if dynamics are time-reversible, then the total wave function does periodically return to its initial state. Hence, for each trajectory, the electronic wave function becomes consistent naturally with the current electronic surface, and further corrections to FSSH are unnecessary. FSSH is reliable, however, only for such rare, serendipitous, time-reversible cases. This is a central result of this paper, and it extends earlier results from ref 28.

To reiterate, adding decoherence is unnecessary only when the entire system—both the nuclear and electronic components—undergo dynamics close to being time reversible. For this to happen, the nuclear dynamics must have a period that is some multiple of the electronic dynamics, or the electronic dynamics must be close to constant. *A priori*, it is fairly difficult to predict whether the periods will align. To provide further evidence for the singular nature of periodic dynamics under FSSH, we consider the drift of $|c_l|^2$ when the left well is replaced with an anharmonic Morse potential. Instead of generating histograms of $|c_l|^2$ at a specific E_i, we look at individual trajectories. For a representative portion of the phase space of initial positions and momenta, we allow a single trajectory to oscillate within the Morse well five times (with the dynamics formally integrated along the adiabats). We then plot the drift in $|c_l|^2$ against the trajectory's initial conditions—this is Figure 4. For comparison, a similar procedure is repeated with the usual harmonic wells, and the result is plotted in Figure 5. Comparing the two, we see that the harmonic well sees large changes in $|c_l|^2$ over a greater region of the sampled initial condition space. Nevertheless, for both potentials, there exist wide bands of initial energies for which the nuclear dynamics do not have the same period as the electronic dynamics. Thus, while time-reversible dynamics can occur, they are rare for both coupled harmonic or anharmonic potentials.

In these calculations, we make use of the Hamiltonian:

$$\mathcal{H} = \begin{pmatrix} D(1 - e^{-\sqrt{\frac{\kappa}{2D}}(x-x_0)})^2 - C & V \\ V & \frac{1}{2}m\omega^2 x^2 - Mx - \epsilon_0 \end{pmatrix} \tag{8}$$

where D is the depth of the well, C is the minimum energy of the well, x_0 is the location of that minimum, and κ is the curvature of the well at its minimum. For our analysis, we simply let $D = 1$, and choose $C = -1/4E_r$, $x_0 = -M/(m\omega^2)$, and $\kappa = m\omega^2$, so that at low energies, the Morse well closely resembles the harmonic well it is replacing. Parameters used to generate Figures 4 and 5 are $E_r = 2.39 \times 10^{-2}$, $kT = 0$, $\epsilon_0 = 2.39 \times 10^{-2}$, $V = 1.0 \times 10^{-4}$, $\omega = 6.64 \times 10^{-4}$, and $m = 29200$ (in atomic units).

4. EXTENSION TO THE ZUSMAN LIMIT

In the context of Marcus theory and rate processes, the Zusman result[51−61] is an important theoretical result against which we can benchmark frictional effects. For the spin-boson model in the overdamped regime ($\gamma \gg (\omega(E_r kT_{\text{eff}})^{1/2})/V$), the Zusman rate for electron transfer is (with large enough energetic barrier[62]):

$$k_{\text{Zusman}}^{-1} = k_{\text{Marcus}}^{-1} + k_D^{-1} \tag{9}$$

where

$$k_{\text{Marcus}} = \frac{|V|^2}{\hbar}\sqrt{\frac{\pi}{E_r kT}}\exp\left(\frac{-U^*(x)}{kT}\right) \tag{10}$$

dx.doi.org/10.1021/jp5011346 | J. Phys. Chem. B XXXX, XXX, XXX−XXX

$$k_D \approx \frac{\omega^2}{\gamma}\sqrt{\frac{U^*(x)}{\pi kT}}\exp\left(\frac{-U^*(x)}{kT}\right) \tag{11}$$

and the activation energy is

$$U^*(x) = \frac{(E_r - \epsilon_0)^2}{4E_r} \tag{12}$$

In effect, the Zusman expression is a combination of the Marcus rate and the analogue of Kramer's turnover theory[53,63] for nonadiabatic problems; one must sum up the time for the electron transfer (Marcus) event plus the time for diffusion past the barrier. For a concise derivation of eq 9, see ref 60. As frictional effects grow ($\gamma \to \infty$), the rate of electron transfer slows down; the systems get stuck either before or near the crossing region and cannot traverse the barrier irreversibly.

With this picture in mind, one might expect that the effects of decoherence would be minimal for very large friction. After all, there is no repeated wave packet bifurcation and separation in this limit; instead, there is just one long sojourn near the top of the activated barrier. Nevertheless, one might expect that decoherence effects *would be* quite visible if we investigate a range of different frictional values. After all, as we have argued, decoherence should be important for small- to medium-ranged γ values, and thus frictional effects will be accentuated by looking at transfer rates as the values of γ move from underdamped to overdamped. Note that Kapral and co-workers have previously investigated this question in a different context (i.e., through the quantum-classical Liouville equation) in refs 64, 65.

To examine these claims about decoherence, in Figure 6, we plot the rate of electron transfer versus the frictional parameter

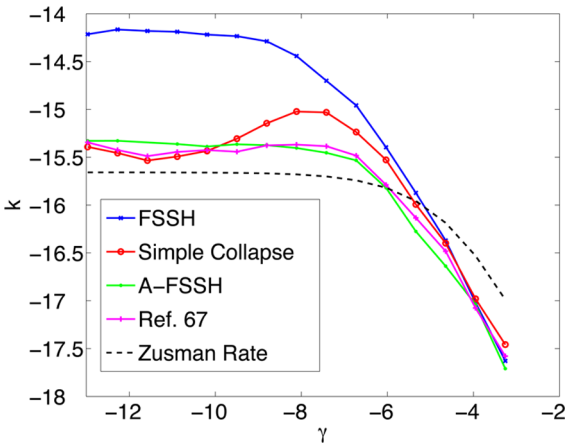

Figure 6. Electron transfer rates from the spin-boson model for a variety of different frictional parameters (γ). Here, standard FSSH is compared against the correct (Zusman) expression and also against three decoherence-improved FSSH algorithms. See text. Note that a naive "simple collapse" implementation of decoherence can give weird, spurious data with artificial oscillations. In order to get reliable data over a broad region of parameter space, a robust decoherence algorithm is needed, e.g. A-FSSH.[27,41] Reference 67 also works well here.

γ. Our parameters are as follows: $E_r = 2.39 \times 10^{-2}$, $kT = 9.5 \times 10^{-4}$, $\epsilon_0 = 1.8 \times 10^{-2}$, $V = 2.5 \times 10^{-5}$, $\omega = 4.375 \times 10^{-5}$, and $m = 1$ (in atomic units). We averaged over 10000 trajectories sampled from an initial Boltzmann distribution, each run with a time step of 1.25. In this figure, we plot results using not only the FSSH algorithm, but also improved FSSH-like algorithms that incorporate decoherence. In particular, we plot rates using three different algorithms for implementing decoherence. The first two of these algorithms we have used previously, and they both are able to recover the correct scaling with V for the spin-boson rate.[39,41] The first approach ("simple collapse") collapses the FSSH electronic wave function[66] each time that a trajectory crosses the minimum of the left-hand well. The second approach ("A-FSSH") is our recent algorithm that propagates the first-order position and momentum moments for each electronic surface and then collapses the electronic wave function—just when the relevant wavepackets must necessarily separate on different electronic surfaces (even for a nuclear wavepacket width that maximizes coherence). For details on the A-FSSH algorithm, see refs 27 and 41. We compare these two algorithms with a third algorithm from Granucci and co-workers[67] that incorporates a decoherence time τ_D, in accordance with ref 36, that is inversely proportional to the adiabatic energy difference and depends on the ratio of the kinetic energy and a parameter C that is chosen to be 0.1 hartree:

$$\tau_D = \frac{\hbar}{|V_2 - V_1|}\left(1 + \frac{C}{E_{\text{kin}}}\right) \tag{13}$$

As one might expect, according to Figure 6, we find that the effects of decoherence are indeed small when frictional damping is overwhelming. All four rates are all equivalent for large γ, and they are close to the Zusman result. For somewhat smaller (almost overdamped) frictional values, however, several points should be made. First, note that FSSH predicts an electron transfer rate that is too large; this is mostly corrected by all methods that add decoherence. We documented this erroneous behavior for surface hopping (without decoherence) a few years ago.[39,41] Second, notice that the simple-collapse method yields completely artificial oscillations in the rate of electron transfer as a function of γ. This spurious behavior is the result of our implementing a naive (and simple-minded) "simple-collapse" scheme. Namely, because the simple-collapse scheme implements a decoherence event only when the particle reaches the bottom of the well, this scheme is bound to fail when trajectories do not make it all the way to the bottom of the well (as would happen in the case of medium-to-large friction). Thus, the simple-collapse data is not qualitatively correct as a function of γ. The decoherence method from ref 67 agrees more or less with A-FSSH for much of the range of γ. We believe eq 13 performs well here because electron transfer in the Zusman regime does not require an accurate treatment of coherence and, in our experience, the Granucci method yields a decoherence rate that tends to overestimate the true rate. For example, the decoherence rate in eq 13 destroys the coherence between two wavepackets on parallel surfaces, which is not physical. For a numerical example, see the Appendix.

In the end, the lesson of Figure 6 is clear; while decoherence is crucial for correcting FSSH and obtaining accurate kinetic and dynamic data, such a decoherence correction must be well-derived and robust. A naive approach (like simple collapse) for decoherence cannot be used to study frictional effects in electron transfer processes.

5. CONCLUSION

In this paper, we have shown that only with zero friction and at certain initial energies are the dynamics simulated by FSSH

dx.doi.org/10.1021/jp5011346 | J. Phys. Chem. B XXXX, XXX, XXX−XXX

time-reversible, and hence, accounting for decoherence is unnecessary only in these situations. In all other circumstances, the value of the electronic wave function is not periodic, and FSSH is unable to recover the correct V^2 scaling. The result from Sibert et al. is then a rare occurrence; very few parameter regimes and initial conditions are time-reversible under FSSH, and as soon as the dynamics become time-irreversible, FSSH accuracy decreases. Furthermore, the method by which we account for decoherence also has a significant effect on the calculated outcome. We conclude that, in almost all circumstances, modeling decoherence correctly for FSSH is necessary to obtain accurate results for nonadiabatic problems with strongly avoided crossings, including spin-boson systems.

APPENDIX

To show that the approach proposed in ref 67 overestimates the true decoherence rate, in Figure 7 we plot the transmission

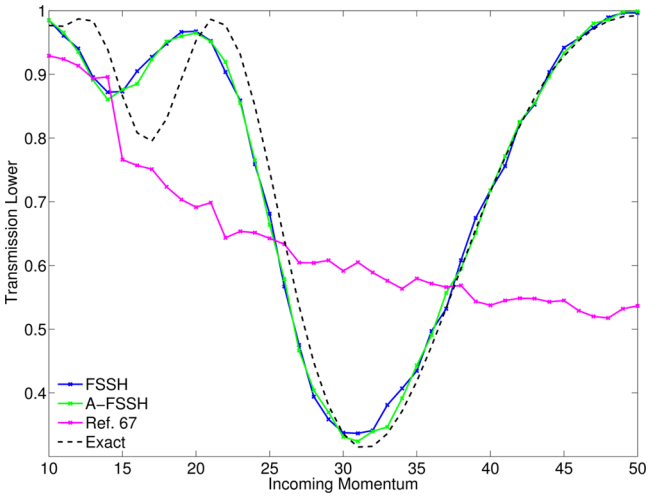

Figure 7. Transmission on the lower adiabatic surface as a function of incoming momentum for the second Tully problem. Parameters are those used in ref 18.

as a function of incoming momentum for the well-known second Tully problem.[18] Note that ref 67 does not recover the correct Stueckelberg oscillations here, even though FSSH and A-FSSH do recover such behavior. Nevertheless, for the Zusman problem, branching ratios are not as sensitive to the precise treatment of electronic coherence, which likely helps to explain why the decoherence scheme in eq 13 (from ref 67) yields an accurate result in Figure 6.

AUTHOR INFORMATION

Corresponding Author

*E-mail: landrybr@gmail.com.

Notes

The authors declare no competing financial interest.

ACKNOWLEDGMENTS

This work was supported by the Air Force Office of Science Research PECASE award under AFOSR Grant No. FA9550-13-1-0157. J.E.S. also acknowledges an Alfred P. Sloan Research Fellowship and a David and Lucille Packard Fellowship. The authors thank Kousik Samanta for helpful discussions regarding ref 67.

REFERENCES

(1) Sugita, Y.; Okamoto, Y. Replica-exchange molecular dynamics method for protein folding. *Chem. Phys. Lett.* **1999**, *314*, 141−151.
(2) Karplus, M.; McCammon, J. A. Molecular dynamics simulations of biomolecules. *Nat. Struct. Biol.* **2002**, *9*, 646−652.
(3) A. Liwo, M. K.; Scheraga, H. A. Ab initio simulations of protein-folding pathways by molecular dynamics with the united-residue model of polypeptide chains. *Proc. Nat. Acad. Sci. U.S.A.* **2005**, *102*, 2362−2367.
(4) Heyes, D. M.; Morriss, G. P.; Evans, D. J. Nonequilibrium molecular dynamics study of shear flow in soft disks. *J. Chem. Phys.* **1985**, *83*, 4760.
(5) Bordat, P.; Müller-Plathe, F. The shear viscosity of molecular fluids: A calculation by reverse nonequilibrium molecular dynamics. *J. Chem. Phys.* **2002**, *116*, 3362.
(6) Müller, T. J.; Al-Samman, M.; Müller-Plathe, F. The influence of thermostats and manostats on reverse nonequilibrium molecular dynamics calculations of fluid viscosities. *J. Chem. Phys.* **2008**, *129*, 014102.
(7) Hammes-Schiffer, S.; Soudackov, A. V. Proton-coupled electron transfer in solution, proteins, and electrochemistry. *J. Phys. Chem. B* **2008**, *112*, 14108−14123.
(8) Wodtke, A. M.; Tully, J. C.; Auerbach, D. J. Electronically non-adiabatic interactions of molecules at metal surfaces: Can we trust the Born Oppenheimer approximation for surface chemistry? *Int. Rev. Phys. Chem.* **2004**, *23*, 513.
(9) Stock, G.; Thoss, M. Semiclassical description of nonadiabatic quantum dynamics. *Phys. Rev. Lett.* **1997**, *78*, 578.
(10) Ben-Nun, M.; Quenneville, J.; Martinez, T. J. Ab initio multiple spawning: Photochemistry from first principles quantum molecular dynamics. *J. Phys. Chem. A* **2000**, *104*, 5161−5175.
(11) Ben-Nun, M.; Martinez, T. J. A continuous spawning method for nonadiabatic dynamics and validation for the zero temperature spin boson problem. *Isr. J. Chem.* **2007**, *47*, 75.
(12) Kapral, R.; Ciccotti, G. Mixed quantum-classical dynamics. *J. Chem. Phys.* **1999**, *110*, 8919−8929.
(13) Hsieh, C.; Kapral, R. Nonadiabatic dynamics in open quantum-classical systems: Forward-backward trajectory solution. *J. Chem. Phys.* **2012**, *137*, 22A507.
(14) Saita, K.; Shalashilin, D. V. On-the-fly ab initio molecular dynamics with multiconfigurational Ehrenfest method. *J. Chem. Phys.* **2012**, *137*, 22A506.
(15) Webster, F.; Wang, E. T.; Rossky, P. J.; Friesner, R. A. Stationary phase surface hopping for nonadiabatic dynamics: Two-state systems. *J. Chem. Phys.* **1994**, *100*, 4835−4847.
(16) Fischer, S. A.; Chapman, C. T.; Li, X. Surface hopping with Ehrenfest excited potential. *J. Chem. Phys.* **2011**, *135*, 144102.
(17) Huo, P.; Miller, T. F., III; Coker, D. F. Communication: Predictive partial linearized path integral simulation of condensed phase electron transfer dynamics. *J. Chem. Phys.* **2013**, *139*, 151103.
(18) Tully, J. C. Molecular dynamics with electronic transitions. *J. Chem. Phys.* **1990**, *93*, 1061−1071.
(19) Hazra, A.; Soudackov, A. V.; Hammes-Schiffer, S. Role of solvent dynamics in ultrafast photoinduced proton-coupled electron transfer reactions in solution. *J. Phys. Chem. B* **2010**, *114*, 12319−12332.
(20) Nachtigallova, D.; Aquino, A. J. A.; Szymczak, J. J.; Barbatti, M.; Hobza, P.; Lischka, H. Nonadiabatic dynamics of uracil: population split among different decay mechanisms. *J. Phys. Chem. A* **2011**, *115*, 5247−5255.
(21) Hudock, H. R.; Levine, B. G.; Thompson, A. L.; Satzger, H.; Townsend, D.; Gador, N.; Ullrich, S.; Stolow, A.; Martinez, T. J. Ab initio molecular dynamics and time-resolved photoelectron spectroscopy of electronically excited uracil and thymine. *J. Phys. Chem. A* **2007**, *111*, 8500.
(22) Jiang, R.; Sibert, E. L. Surface hopping simulation of vibrational predissociation of methanol dimer. *J. Chem. Phys.* **2012**, *136*, 224104.
(23) Topaler, M. S.; Allison, T. C.; Schwenke, D. W.; Truhlar, D. G. Test of trajectory surface hopping against accurate quantum dynamics

for an electronically nonadiabatic chemical reaction. *J. Phys. Chem. A* **1998**, *102*, 1666−1673.
(24) Hack, M. D.; Wensmann, A. M.; Truhlar, D. G.; Ben-Nun, M.; Martinez, T. J. Comparison of full multiple spawning, trajectory surface hopping, and converged quantum mechanics for electronically nonadiabatic dynamics. *J. Chem. Phys.* **2001**, *115*, 1172−1186.
(25) Muller, U.; Stock, G. Surface-hopping modeling of photoinduced relaxation dynamics on coupled potential-energy surfaces. *J. Chem. Phys.* **1997**, *107*, 6230.
(26) Fang, J. Y.; Hammes-Schiffer, S. Improvement of the internal consistency in trajectory surface hopping. *J. Phys. Chem. A* **1999**, *103*, 9399−9407.
(27) Subotnik, J. E.; Shenvi, N. A new approach to decoherence and momentum rescaling in the surface hopping algorithm. *J. Chem. Phys.* **2011**, *134*, 024105.
(28) Subotnik, J. E.; Shenvi, N. Decoherence and surface hopping: When can averaging over initial conditions help capture the effects of wave packet separation? *J. Chem. Phys.* **2011**, *134*, 244114.
(29) Schwartz, B. J.; Bittner, E. R.; Prezhdo, O. V.; Rossky, P. J. Quantum decoherence and the isotope effect in condensed phase nonadiabatic molecular dynamics simulations. *J. Chem. Phys.* **1996**, *104*, 5942.
(30) Prezhdo, O. V.; Rossky, P. J. Mean-field molecular dynamics with surface hopping. *J. Chem. Phys.* **1997**, *107*, 825−834.
(31) Larsen, R. E.; Bedard-Hearn, M. J.; Schwartz, B. J. Exploring the role of decoherence in condensed-phase nonadiabatic dynamics: A comparison of different mixed quantum/classical simulation algorithms for the excited hydrated electron. *J. Phys. Chem. B* **2006**, *110*, 20055−20066.
(32) Bedard-Hearn, M. J.; Larsen, R. E.; Schwartz, B. J. Mean-field dynamics with stochastic decoherence (MF-SD): A new algorithm for nonadiabatic mixed quantum/classical molecular-dynamics simulations with nuclear-induced decoherence. *J. Chem. Phys.* **2005**, *123*, 234106.
(33) Zhu, C.; Jasper, A. W.; Truhlar, D. G. Non-Born-Oppenheimer trajectories with self-consistent decay of mixing. *J. Chem. Phys.* **2004**, *120*, 5543−5547.
(34) Zhu, C.; Nangia, S.; Jasper, A. W.; Truhlar, D. G. Coherent switching with decay of mixing: An improved treatment of electronic coherence for non-Born-Oppenheimer trajectories. *J. Chem. Phys.* **2004**, *121*, 7658−7670.
(35) Jasper, A. W.; Truhlar, D. G. Electronic decoherence time for non-Born-Oppenheimer trajectories. *J. Chem. Phys.* **2005**, *123*, 064103.
(36) Zhu, C.; Jasper, A. W.; Truhlar, D. G. Non-Born-Oppenheimer Liouville-von Neumann dynamics. Evolution of a subsystem controlled by linear and population-driven decay of mixing with decoherent and coherent switching. *J. Chem. Theory Comp.* **2005**, *1*, 527−540.
(37) Jasper, A. W.; Truhlar, D. G. Non-Born Oppenheimer molecular dynamics of Na···FH photodissociation. *J. Chem. Phys.* **2007**, *127*, 194306.
(38) Shenvi, N.; Subotnik, J. E.; Yang, W. Simultaneous-trajectory surface hopping: A parameter-free algorithm for implementing decoherence in nonadiabatic dynamic. *J. Chem. Phys.* **2011**, *134*, 144102.
(39) Landry, B. R.; Subotnik, J. E. Standard surface hopping predicts incorrect scaling for Marcus golden-rule rate: The decoherence problem cannot be ignored. *J. Chem. Phys.* **2011**, *135*, 191101.
(40) The full expression for the Marcus charge transfer rate is given as

$$k = \frac{2\pi |V|^2}{\hbar\sqrt{4\pi E_r kT}} \exp\left(-\frac{(E_r - \epsilon_0)^2}{4E_r kT}\right) \quad (14)$$

where the variables are the standard spin-boson parameters. In this paper we focus on the ability of surface hopping algorithms to recover the scaling of the result with respect to V, while noting that previous studies have investigated the scaling of k with e_0 (ref 41) and T (ref 68) as well.
(41) Landry, B. R.; Subotnik, J. E. How to recover Marcus theory with fewest switches surface hopping: Add just a touch of decoherence. *J. Chem. Phys.* **2012**, *137*, 22A513.
(42) Leggett, A. J.; Chakravarty, S.; Dorsey, A. T.; Fisher, M. P. A.; Garg, A.; Zwerger, W. Dynamics of the dissipative two-state system. *Rev. Mod. Phys.* **1987**, *59*, 1−85.
(43) Mac Kernan, D.; Ciccotti, G.; Kapral, R. Surface-hopping dynamics of a spin-boson system. *J. Chem. Phys.* **2002**, *116*, 2346−2353.
(44) Schwerdtfeger, C. A.; Soudackov, A. V.; Hammes-Schiffer, S. Nonadiabatic dynamics of electron transfer in solution: Explicit and implicit solvent treatments that include multiple relaxation time scales. *J. Chem. Phys.* **2014**, *140*, 034113.
(45) Cline, R. E.; Wolynes, P. G. Stochastic dynamic models of curve crossing phenomena in condensed phases. *J. Chem. Phys.* **1987**, *86*, 3836−3844.
(46) Warshel, A.; Hwang, J. K. Simulation of the dynamics of electron transfer reactions in polar solvents: Semiclassical trajectories and dispersed polaron approaches. *J. Chem. Phys.* **1986**, *84*, 4938−4957.
(47) Mukamel, S. *Nonlinear Optical Spectroscopy*; Oxford University Press: New York, 1999.
(48) Xie, W.; Baj, S.; Zhu, L.; Shi, Q. Calculation of electron transfer rates using mixed quantum classical approaches: Nonadiabatic limit and beyond. *J. Phys. Chem. A* **2013**, *117*, 6196−6204.
(49) Landry, B. R.; Falk, M. J.; Subotnik, J. E. The correct interpretation of surface hopping trajectories: How to calculate electronic properties. *J. Chem. Phys.* **2013**, *139*, 211101.
(50) Subotnik, J. E.; Ouyang, W.; Landry, B. R. Can we derive Tully's surface-hopping algorithm from the semiclassical quantum Liouville equation? Almost, but only with decoherence. *J. Chem. Phys.* **2013**, *139*, 214107.
(51) Tully, J. C.; Gilmer, G. H.; Shugard, M. Molecular dynamics of surface diffusion. I. The motion of adatoms and clusters. *J. Chem. Phys.* **1979**, *71*, 1630−1642.
(52) Beeman, D. Some multistep methods for use in molecular dynamics calculations. *J. Comput. Phys.* **1976**, *71*, 1630−1642.
(53) Nitzan, A. *Chemical Dynamics in Condensed Phases*; Oxford University Press: New York, 2006.
(54) We have energy conservation in the zero stochasticity limit, hence $E_i + E_{min} = 1/2mv^2 + 1/2m\omega^2x^2 + Mx$ for all trajectories on the left diabatic well, where $E_{min} = -1/4E_r$, the minimum energy of the left diabatic well. (Recall we defined E_i relative to this minimum energy.) At the avoided crossing, $1/2m\omega^2x^2 + Mx = 1/2m\omega^2x^2 - Mx - \epsilon_0$; thus, for small V the avoided crossing is located at approximately $x = -\epsilon_0/2M$. This implies $v = ((1/m)(2(E_i - 1/4E_r) - (\epsilon_0)/(2E_r)\epsilon_0 + \epsilon_0)^{1/2}$ at the avoided crossing. For situations with no stochastic forces, the term $|F_l - F_r|$ is $|m\omega^2x + M - m\omega^2x + M| = 2M$. Thus, $v|F_l - F_r| = 2\omega((1/m)(2(E_i - 1/4E_r) - (\epsilon_0)/(2E_r)\epsilon_0 + \epsilon_0))^{1/2}((1/2)E_rm)^{1/2} = \omega(4(E_i - (1/4)E_r)E_r - (\epsilon_0^2) + 2\epsilon_0E_r)^{1/2}$ and $\alpha_{LZ} = (2\pi V^2)/(\hbar\omega(4(E_i - (1/4)E_r)E_r + 2\epsilon_0E_r - (\epsilon_0^2)^{1/2})$.
(55) Hynes, J. T. Outer-sphere electron transfer reactions and frequency-dependent friction. *J. Phys. Chem.* **1986**, *90*, 3701−3706.
(56) Garg, A.; Onuchic, J. N.; Ambegaokar, V. Effect of friction on electron transfer in biomolecules. *J. Chem. Phys.* **1985**, *83*, 4491−4503.
(57) Rips, I.; Jortner, J. Dynamic solvent effects on outersphere electron transfer. *J. Chem. Phys.* **1987**, *87*, 2090−2104.
(58) Rips, I.; Jortner, J. Activationless solvent controlled electron transfer. *J. Chem. Phys.* **1988**, *88*, 818−822.
(59) Zusman, L. D. Outer-sphere electron transfer in polar solvents. *Chem. Phys.* **1980**, *49*, 295−304.
(60) Morillo, M.; Cukier, R. I. The transition from nonadiabatic to solvent controlled adiabatic electron transfer kinetics: The role of quantum and solvent dynamics. *J. Chem. Phys.* **1988**, *89*, 6736−6743.
(61) Yang, D. Y.; Cukier, R. I. The transition from nonadiabatic to solvent controlled adiabatic electron transfer: Solvent dynamical effects in the inverted regime. *J. Chem. Phys.* **1989**, *91*, 281−292.
(62) For an electron transfer event without a large barrier, one must substitute Equation 11 by

$$k_D^{-1} = \frac{2\gamma}{\omega^2}\exp\left(\frac{U(x^*)}{kT}\right)I(x^*) \tag{15}$$

where x^* is the diabatic crossing point and

$$I(x) = \int_0^1 \frac{1}{1-z^2}\,\mathrm{d}z\left(\sqrt{\frac{(z+1)^2}{4z}}\exp\left(-\frac{m\omega^2x^2z}{2kT}\right) - \exp\left(\frac{-m\omega^2x^2}{2kT}\right)\right) \tag{16}$$

See ref 60. In the limit of a large barrier, i.e. $U(x^*) = (m\omega^2(x^*)^2)/2 \gg kT$, Eqn. 15 reduces to eq 11.

(63) Kramers, H. A. Brownian motion in a field of force and the diffusion model of chemical reactions. *Physica* **1940**, *7*, 284−304.

(64) Sergi, A.; Kapral, R. Quantum-classical dynamics of nonadiabatic chemical reactions. *J. Chem. Phys.* **2003**, *118*, 8566.

(65) Sergi, A.; Kapral, R. Nonadiabatic reaction rates for dissipative quantum-classical systems. *J. Chem. Phys.* **2003**, *119*, 12776.

(66) A collapse event is defined by setting

$$\begin{pmatrix} c_1 \\ c_2 \end{pmatrix} \rightarrow \begin{pmatrix} 1 \\ 0 \end{pmatrix} \text{ or } \begin{pmatrix} 0 \\ 1 \end{pmatrix} \tag{17}$$

depending on whether the active surface is the first or second adiabat.

(67) Granucci, G.; Persico, M. Critical appraisal of the fewest switches algorithm for surface hopping. *J. Chem. Phys.* **2007**, *126*, 134114.

(68) Wang, L.; Beljonne, D. Charge transport in organic semiconductors: Assessment of the mean field theory in the hopping regime. *J. Chem. Phys.* **2013**, *139*, 064316.